Journal of Ceramic Processing Research. Vol. 14, No. 4, pp. 577~582 (2013)

J O U R N A L O F
Ceramic Processing Research

Effects of temperature and pressure on properties of SiC–ZrB_2 composites prepared by spark plasma sintering

Jung-Hoon Lee[a], Beom-Soo Jin[a], Myeong-Kyun Kang[a], In-Yong Kim[b], An-Gyun Jeon[c], Jin-Hyoung Park[a], Dong-Ki Kim[d] and Yong-Deok Shin[a,*]

[a]*Wonkwang Univ., 344-2, Sinyong-dong, Iksan-si, Jeonbuk 570-749, Korea*
[b]*Korea Institute of Nuclear Safety, 34, Gwahak-ro,Yuseong-gu, Daejeon 305-338, Korea*
[c]*Honam Univ., 417, Eodeungdae-ro, Gwangsan-gu, Gwangju 560-714, Korea*
[d]*JMC, 817, Palbok-dong 2-ga, Deokjin-gu, Jeonju-si, Jeonbuk 561-844, Korea*

Silicon carbide (SiC)-zirconium diboride (ZrB_2) composites are produced by subjecting a 60 : 40 vol% mixture of β-SiC powder and ZrB_2 matrix to spark plasma sintering (SPS). Sintering is carried out for 60 sec at temperatures of 1400 °C and 1500 °C and uniaxial pressures of 40 MPa, 50 MPa, and 60 MPa, under argon atmosphere. The physical, mechanical, and electrical properties of the sintered SiC-ZrB_2 composites are examined. Evidence of reactions between β-SiC and ZrB_2 in the SiC-ZrB_2 composites sintered under argon atmosphere is not observed by high-resolution x-ray diffraction (HR-XRD) analysis. The trends in the apparent density and flexural strength of the sintered SiC-ZrB_2 composites are not dependent on the uniaxial pressure when the sintering temperature is 1500 °C. Among the sintered SiC-ZrB_2 composites, the specimen produced at 1500 °C and 50 MPa shows the lowest volume electrical resistivity at room temperature, $0.617 \times 10^{-3}\ \Omega \cdot$ cm. By energy-dispersive spectroscopy (EDS) mapping, it is confirmed that ZrB_2-chain formation in the sintered SiC-ZrB_2 composites uniformly occurred at 1500 °C and 50 MPa. The flexural strength of the sintered SiC-ZrB_2 composites is dependent upon their apparent density, but the volume electrical resistivity is independent of the apparent density. Densification of a sintered SiC-ZrB_2 composite through hot pressing is dependent on the sintering temperature and pressure. However, this study confirms that the densification of SiC-ZrB_2 composites through SPS does not depend on the uniaxial pressure.

Key words: Spark plasma sintering (SPS), Uniaxial pressure, Positive temperature coefficient resistance (PCTR), Sintering temperature.

Introduction

Silicon carbide (SiC), with its high melting point of 2800 °C, is a thermochemically stable IV-IV-compound semiconductor. In addition, because of its low coefficient of thermal expansion (ap-proximately 4.36×10^{-6}/°C at 20 ~ 1000 °C), thermal conductivity, thermal impact resistance, strength, and oxidation resistance, SiC is considered to be an outstanding semiconductor [1, 2]. However, owing to the low efficiency of diffusion caused by the strong covalent bond between Si and C, it is difficult to obtain sinter density without sinter additives. In addition, at temperatures below 1000 °C, the electrical resistivity of SiC is considered to have a negative temperature coefficient of resistance (NTCR), causing its temperature to increase and conductivity to become uncontrollable, eventually resulting in overheating [2-4].

Zirconium diboride (ZrB_2), a transition-metal boride, has a hexagonal close packed (HCP) crystal structure of the AlB_2 type. It is composed of an alternating sequence (MBMBMB) of metal atoms (M) and graphite-like boron (B). In this type of structure, there are strong boron-boron and metal-boron covalent bonds, as well as distinctive bonds with the characteristics of metallic bonds [2]. However, when ZrB_2 is employed as an electrical conduction material at temperatures in excess of 1000 °C, problems arise because of its poor hardness and internal oxidation resistance [5].

Dispersion of ZrB_2 or other metal borides in SiC-based matrices was found to be useful in the production of materials for heaters and igniters on the basis of their adequate resistivity, positive temperature coefficient of resistance (PTCR), greater strength and toughness compared to the matrix SiC, and good oxidation resistance at temperatures up to ap-proximately 1200 °C [6]. Therefore, the combination of SiC and ZrB_2 results in a SiC-ZrB_2 composite with high electrical conductivity, superior oxidation resistance, and high mechanical strength, which can be used as a conduction material or ohmic contact electrode at high and low temperatures [2].

The general method of producing a SiC ceramic is via hot pressing(HP), a solid-state sintering process, at temperatures of ap-proximately 1950 ~ 2100 °C. Liquid-phase sintering (e.g., addition of Al_2O_3 and

*Corresponding author:
Tel : +82-63-850-6736
Fax: +82-63-850-7315
E-mail: ydshin@wku.ac.kr

Y_2O_3) has been employed to lower the temperature of the HP process to below 1950 °C [7].

Although spark plasma sintering (SPS) is similar to HP, there are some significant differences between them: application of an electric field to both upper and lower electrodes and sintering of materials within the powders by direct heating are typical to SPS. However, despite many experimental studies, the density parameter of the sintered compacts is still unclear, which results in a limitation in systematic examinations.

In the current study experiment, SPS was employed to obtain a ceramic composite of SiC-ZrB_2, a high-density sintered compact, at temperatures of 1400 °C or 1500 °C (ap-proximately 450 ~ 700 °C lower than that required for HP). In order to analyze the physical, mechanical, and electrical properties of the SiC-ZrB_2 composite sintered via SPS, the apparent density, flexural strength, volume electrical resistivity, high-resolution x-ray diffraction (HR-XRD), x-ray photoelectron spectroscopy (XPS), field-emission scanning electron microscopy (FE-SEM), and energy-dispersive spectroscopy (EDS)were examined.

Experimental Procedure

Powder preparation

High-purity β-SiC (Grade BF12, H. C. Starck, Germany) and ZrB_2 (Grade B, H. C. Starck, Germany) were used as the starting materials. β-SiC and ZrB_2 were combined in the ratio 60 : 40 vol%. The measured materials were combined with distilled water in a polyurethane bowl (volume: 1583.4 ml). They were then subjected to the planetary ball mill process with high-purity SiC balls (ball diameters: 10 mm and 20 mm, with the number of SiC balls in 1 : 5 ratio), for 24 hrs. Next, the powders were dehydrated by heating for 12 hrs at 100 °C and sieved through a 60-mesh screen.

Sintering process

The dried powders were put in a graphite die with an inner diameter of 20 mm, enclosed with graphite foil, and sintered using a PAS-H3000 apparatus (ElTek Co. Ltd, Korea) at sintering temperatures of 1400 °C and 1500 °C and uniaxial pressures of 40 MPa, 50 MPa, and 60 MPa, under argon atmosphere. The sintered composites were classified according to their sintering conditions (Table 1).

Evaluation of physical properties

Theoretical densities of the SiC-ZrB_2 composites were calculated on the basis of the rule of mixtures (3.217 g/cm^3 for β-SiC and 6.085 g/cm^3 for ZrB_2). The final SiC-ZrB_2 composites (the sintered compacts) were ground with a diamond wheel and shaped into disks. Then the apparent density of each of the SiC-ZrB_2 composite specimens was measured 10 times by the Archimedes method. The disks were machined to obtain SiC-ZrB_2 composite bars with dimensions of 1.0 × 0.7 × 10 mm^3. The bars were polished using 1 μm diamond paste and beveled at 45° for mechanical testing (ASTM F394-78).

Table 1. SiC-ZrB_2 composites

Pressure (MPa) Temperature(°C)	40	50	60
1400	TP144	TP145	TP146
1500	TP154	TP155	TP156

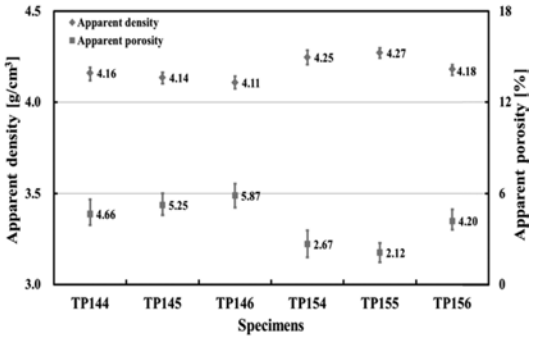

Fig. 1. Apparent density of the sintered SiC–ZrB_2 composites.

The three-point flexural strength of each sintered SiC-ZrB_2 compacts were measured ap-proximately 5-6 times at room temperature using a material test apparatus (Model 4204, Instron, USA) under the following conditions: outer span, 10 mm; inner span, 8 mm; and crosshead speed, 0.07 mm/min.

The microstructures of a fracture surface of a flexural strength test specimen were observed using FE-SEM (S-4800, Hitachi, Japan). EDS mapping(S-4800, Horiba, Japan) was carried out to analyze the atom distribution in the specimens. Atom and phase analysis of the sintered SiC-ZrB_2 compacts was performed by HR-XRD (X'Pert PRO MRD, PANalytical B.V., The Netherlands) and XPS (K-Alpha ESKA SYSTEM, Thermo Electron Corp., UK), respectively.

The sintered SiC-ZrB_2 compacts were cut by wire electrical discharge machining (WEDM, α-OPiB, FANAC, Japan) to produce specimens for volume electrical resistivity measurements. The volume electrical resistivity of each specimen processed by WEDM was measured 200 times by the Pauw method [8]. During the measurements, the temperature was increased from room temperature to 500 °C.

Results and Discussion

Apparent density

As demonstrated in Fig. 1, at a sintering temperature of 1400 °C, the apparent density of the sintered SiC-ZrB_2 composites decreased as the uniaxial pressure increased. This was not in accordance with the general phenomenon of HP. It is hypothesized that as the

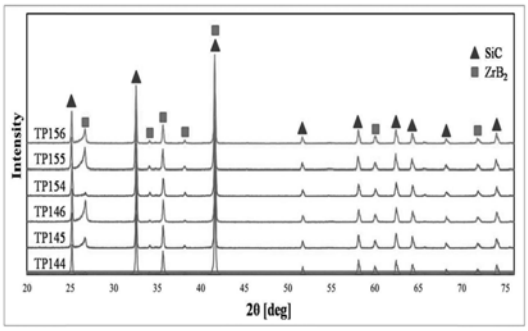

Fig. 2. High-resolution x-ray diffraction pattern of the sintered SiC–ZrB_2 composites.

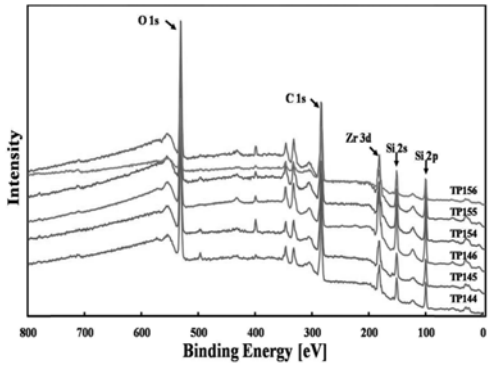

Fig. 3. X-ray photoelectron spectrum of the sintered SiC-ZrB_2 composites.

uniaxial pressure in SPS increases, the neck cross-sectional area between particles is extended and that the resistance of this area is lowered. This leads to a reduction in Joule heating in the neck cross-sectional areas [7]. By contrast, at a sintering temperature of 1500 ºC, the apparent density of the sintered SiC-ZrB_2 composites were not dependent on the uniaxial pressure and the sintered compact TP155 had the highest apparent density. The apparent density of TP154 was lower than that of TP155. It is hypothesized that sparking in SPS and self-Joule heating were suppressed in the sintering powder section because the current density in the mold section was higher than that in the sintering powder section at a sintering temperature of 1500 ºC.

Phase analysis and microstructure

The HR-XRD analysis of the sintered SiC-ZrB_2 composites is shown in Fig. 2. All the peak values appear on an International Centre for Diffraction Data (ICDD) card, with the following code numbers: 00-029-1128(SiC), 01-074-1302(SiC), 00-042-1091(SiC), and 01-075-0964(ZrB_2). No evidence of reactions between β-SiC and ZrB_2 in the SiC-ZrB_2 composites sintered under argon atmosphere was observed in the HR-XRD analysis.

In order to analyze the bonds between the atoms, the polished surfaces of the sintered SiC-ZrB_2 composites were examined using XPS. Si, Zr, C, and O atoms

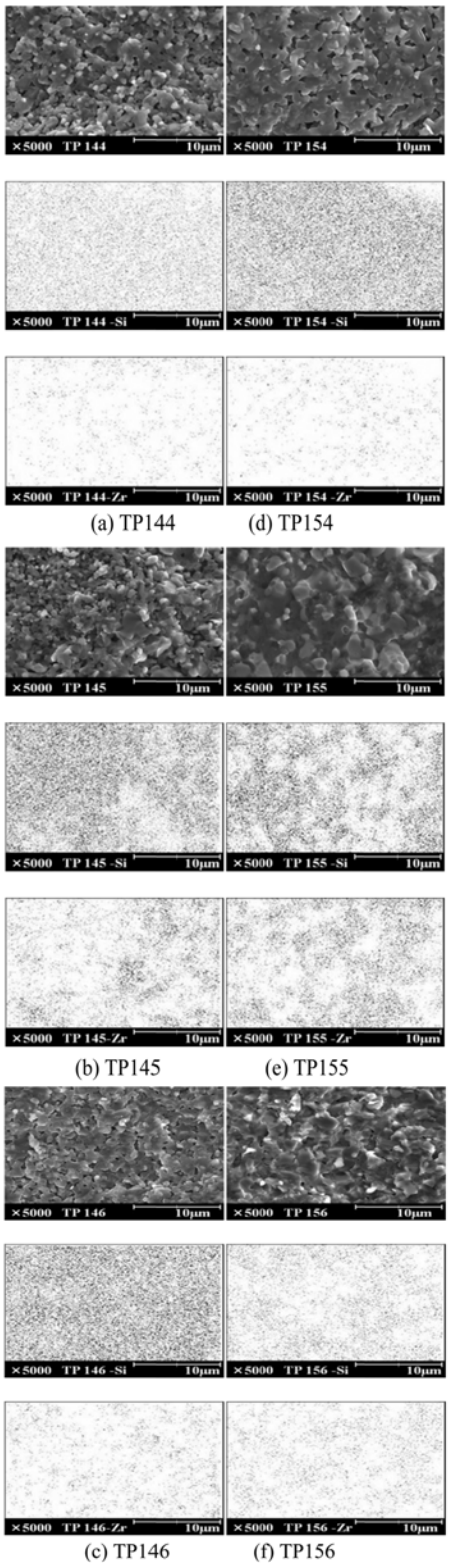

Fig. 4. Field-emission scanning electron microscopy images and energy-dispersive spectroscopy mapping of the sintered SiC-ZrB_2 composites.

were observed in the polished surfaces of all the sintered SiC-SZrB_2 composite specimens, as demonstrated in Fig.3. SiC and ZrB_2 phases were observed via HR-XRD analysis. The microstructure of a fractured

surface of the sintered compact TP155, observed using FE-SEM, revealed the lowest apparent porosity (2.12%), as shown in Fig. 4. The distribution of Zr in the sintered compact TP155, observed using EDS mapping, revealed the higher than that of TP154 and TP156. It is hypothesized that internal temperature of the sintered compact TP155 was locally increased owing to the thermal diffusion induced by Joule heating and SPS.

Mechanical properties

In the literature, the flexural strength of a given ceramic is related to grain growth, which in turn is sensitive to heat. Therefore, when the microstructure of the ceramic becomes coarse and phase-shaped upon annealing, the fracture toughness of the ceramic increases, while the flexural strength decreases [9-11]. However, with the second phase composition and proper annealing, the ceramic microstructure becomes more stable and reduction in the flexural strength is prevented. The factor that affects the mechanical strength of ceramic composites is $\sigma = \sigma_0 \exp(-k\alpha)$, where σ_0 is the flexural strength of a defect-free material, α is the residual porosity, and k is a constant [12]. The flexural strength of the sintered SiC-ZrB_2 composites (Fig. 5) is strongly dependent on the apparent density (Fig. 1) because the flexural strength decreases as the apparent porosity increases. The apparent porosity can be reconfirmed from the FE-SEM images of fracture surfaces of the sintered SiC-ZrB_2 composites (Fig. 4). The flexural strengths of the sintered SiC-ZrB_2 composites, ap-proximately 207.46-460.42 MPa at room temperature (Fig. 5), were lower than those of single-crystal SiC and ZrB_2 without porosity (ap-proximately 350-500 MPa and 512-618 MPa, respectively) [13, 14]. As demonstrated in Fig. 5, the sintered compact TP155 has the highest flexural strength, ap-proximately 326.91-460.42 MPa, from among the sintered SiC-ZrB_2 composites. This is because during the sintering process, the amount of the volatile component existed, as the sintered compact TP155 had the lowest apparent porosity (2.12%). In addition, the flexural strength of the sintered compact TP155 was lower than that of TP155 without porosity (414.8-547.2 MPa), according to the expression $\sigma = V_f\sigma_{sic} + (1\text{-}V_f)\sigma_{ZrB2}$ (where V_f is the volume variation of SiC). However, accurate estimation of the porosity is difficult because of the effect of grain growth, formation of phase-shaped grain boundaries upon annealing, and debonding by the combination of liquid phases.

Volume electrical resistivity

The electrical resistivity of SiC single crystals at room temperature is ap-proximately 0.13 Ω・cm. However, when the temperature is increased to 250 °C, the electrical resistivity decreases to 0.1 Ω・cm because of the NTCR; with a further increase in temperature to 900 °C, the resistivity increases to ap-proximately 0.16 Ω・cm because of the PTCR. The electrical resistivity of polycrystalline SiC is in the range 0.1-0.3 Ω・cm at room temperature. However, the electrical resistivity decreases to one-third of the abovementioned value because of the NTCR when the temperature increased to 800 °C. At temperatures above 800 °C, the electrical resistivity increases gradually because of the PTCR. This difference in the behaviors of single-crystal and polycrystalline SiC results from the facts that polycrystalline SiC grains are smaller than SiC single crystals and that polycrystalline SiC has a greater number of grain boundaries than single-crystal SiC. Consequently, the grains in polycrystalline SiC grow in size as the sintering temperature is increased up to 800 °C, causing the electrical resistivity to decrease [15]. The electrical conduction in the case of polycrystalline SiC has been explained on the basis of a band model having electric potential barriers at the grain boundaries. It has been stated that it goes over the electric potential barriers by the high thermal excitation at high temperature, whereas it passes through the electric potential barriers by the tunnel and bulk conduction at low temperature [15]. Fig. 6 shows the electrical resistivities of the sintered SiC-ZrB_2 composites determined by the Pauw method for room temperature, 100 °C, 300 °C, and 500 °C. The average volume electrical resistivity measured at each temperature is shown in this figure. The volume electrical resistivities of the sintered compacts TP144, TP145, TP146, TP154, TP155, and TP156 at room temperature are 2.241×10^{-3}, 0.675×10^{-3}, 0.722×10^{-3}, 1.342×10^{-3}, 0.617×10^{-3}, and 0.671×10^{-3} Ω・cm,

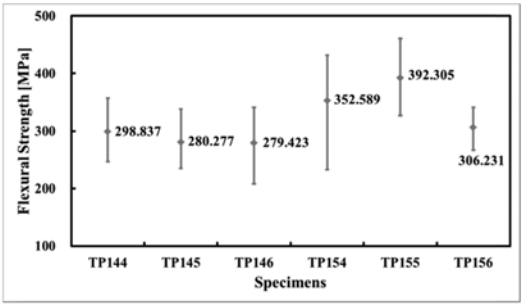

Fig. 5. Three-point flexural strength of the sintered SiC-ZrB_2 com-posites.

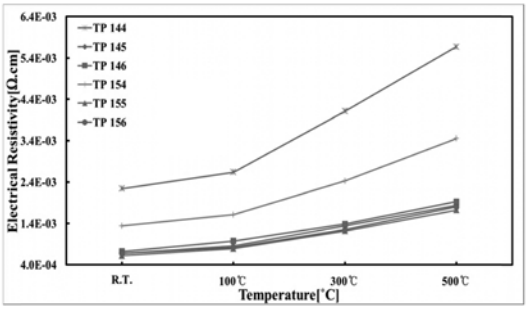

Fig. 6. Volume electrical resistivity of the sintered SiC-ZrB_2 com-posites.

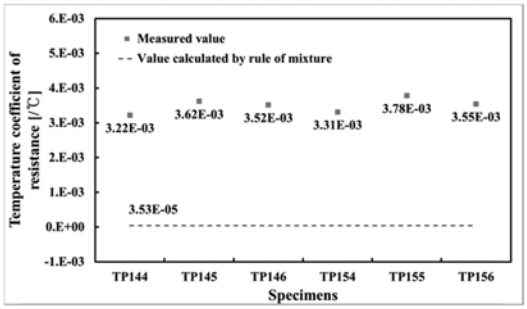

Fig. 7. Temperature coefficient of resistance of the sintered SiC-ZrB_2 composites.

respectively. The volume electrical resistivities of TP144, TP145, TP146, TP154, TP155, and TP156 at 500 ºC are 5.672×10^{-3}, 1.836×10^{-3}, 1.927×10^{-3}, 3.454×10^{-3}, 1.726×10^{-3}, and $1.801 \times 10^{-3}\,\Omega \cdot$ cm, respectively. The electrical conductivity of a transition-metal boride such as ZrB_2 is markedly higher than the electrical resistivity of SiC, which is a semiconductor. Therefore, if the amount of ZrB_2 added to SiC is more than 40 vol%, the volume electrical resistivity of the SiC-ZrB_2 composites depend on the formation of chains of ZrB_2 grains, which have good electrical conductivity. The volume electrical resistivity of the sintered compact TP144 is relatively higher than those of the other SiC-ZrB_2 composites because the frequent generation of spark plasma under the high pulse voltage causes the chains of ZrB_2 grains to break.

The volume electrical resistivities of the sintered compacts TP144, TP145, TP146, TP154, TP155, and TP156 at room temperature (ap-proximately $0.617 \times 10^{-3} \sim 2.241 \times 10^{-3}\Omega \cdot$ cm) are outside the range that would be specified on the basis of Landauer's effective medium theory (ap-proximately $1.49 \times 10^{-4} \sim 4.49 \times 10^{-4}\,\Omega \cdot$ cm) [16, 17]. The volume electrical resistivity of ZrB_2 (ap-proximately $1.5 \times 10^{-5} \sim 4.5 \times 10^{-5}\,\Omega \cdot$ cm) is lower than that of SiC (ap-proximately 0.1-1.8Ω · cm) by a factor of ap-proximately 10^{-5}. Therefore, if the amount of transition-metal compound added to SiC is more than 40 vol%, the effective medium theory does not hold good, and the volume electrical resistivity of the SiC-ZrB_2 composites would depend on the formation of ZrB_2 chains, which have good electrical conductivity. The sintered compact TP155 had the lowest volume electrical resistivity among all the sintered SiC-ZrB_2 composites considered in this study because its distribution of Zr was the highest in this compact, as confirmed by EDS mapping. It is proposed that the optimum uniaxial pressure for the formation of ZrB_2 chains is 50 MPa at sintering temperatures of 1400 ºC and 1500 ºC.

The volume electrical resistivity of the sintered SiC-ZrB_2 composites (Fig. 6) was independent of the apparent density (Fig. 1). Fig. 7 shows the temperature coefficients of resistance (TCRs) of the sintered SiC-ZrB_2 composites, calculated using the rule of mixtures, to be 3.53×10^{-5}/°C; the experimental values were measured by the Pauw method [8, 17]. The TCRs of the sintered compact TP144, TP145, TP146, TP154, TP155, and TP156 were in the range (3.22-3.78)× 10^{-3} ºC, indicating that all the sintered SiC-ZrB_2 composites had a PTCR. The sintered compact TP144 had the lowest PTCR among all the sintered SiC-ZrB_2 composites considered in this study because its ZrB_2 chains were broken by the frequent occurrence of spark plasmas under the high applied pulse voltage.

Conclusion

The components of SiC-ZrB_2 composites, β-SiC and ZrB_2, were combined in the ratio 60 : 40 vol%. The SiC-ZrB_2 composites were prepared by SPS for 60 sec at sintering temperatures of 1400°C and 1500 ºC and uniaxial pressures of 40 MPa, 50 MPa, and 60 MPa, under argon atmosphere. The physical, mechanical, and electrical properties of the sintered SiC-ZrB_2 composites were evaluated. The following results were obtained:

1. The apparent densities of the sintered SiC-ZrB_2 composites were independent of the uniaxial pressure when the sintering temperature was 1400 ºC and 1500 ºC. The sintered compact TP155 had the lowest apparent porosity (2.12%), and TP146 had the highest apparent porosity (5.87%).
2. No evidence of reactions between β-SiC and ZrB_2 in the SiC-ZrB_2 composites sintered under argon atmosphere was observed in HR-XRD analysis.
3. EDS mapping showed that ZrB_2 chain formation in the sintered SiC-ZrB_2 composites uniformly occurred at a sintering temperature and uniaxial pressure of 1500 ºC and 50 MPa, respectively.
4. Among the sintered SiC-ZrB_2 composites, the sintered compact TP155 had the highest flexural strength (ap-proximately 326.91 ~ 460.42 MPa) and TP146 had the lowest flexural strength (ap-proximately 207.46 ~ 340.80 MPa).
5. Among the sintered SiC-ZrB_2 composites, the sintered compact TP155 had the lowest electrical resistivity ($0.617 \times 10^{-3}\,\Omega \cdot$ cm at room temperature) and TP144 had the highest electrical resistivity ($2.241 \times 10^{-3}\Omega \cdot$ cm at room temperature).
6. The volume electrical resistivity of the sintered SiC-ZrB_2 composites was dependent on the formation of ZrB_2 chains, which have good electrical conductivity, and not on the apparent density. However, the flexural strength of the sintered SiC-ZrB_2 composites was strongly dependent on the apparent density.
7. The TCRs of the sintered compact TP144, TP145, TP146, TP154, TP155, and TP156 were in the range $3.22 \times 10^{-3} \sim 3.78 \times 10^{-3}$/ºC, indicating that all the sintered SiC-ZrB_2 composites had a PTCR.

Acknowledgments

This paper was supported by Wonkwang University in 2013.

References

1. P.A. Hoffman, D.J. Creen and J.R. Hellmann, "Thermo elastic properties of silicon carbide-titanium diboride particulate composites", M.S. Thesis, Pennsylvania State University. (1992).
2. J.H. Lee, J.Y. Ju, C.H. Kim and Y.D. Shin, JEET. 6[4] (2011) 543-550.
3. H. Hashiguchi and H.Kimugasa, J. Ceram. Soc. Jpn. 102[2] (1994) 160-164.
4. A.L. Chamberlain, W.G. Fahrenholtz and G.E. Hilmas, J. Eur. Ceram. Soc. 29 (2009) 3401-3408.
5. M. Nakamura, I.Shigematsu, K. Kanayama and Y. Hirai, J. Mater. Sci. 26 (1991) 6078-6082.
6. D. Sciti, C. Melandri and A.Bellosi, Advanced Eng. Mater. 6 [9] (2004) 775-781.
7. Y.D. Shin, J.Y. Ju and T.H. Ko, Trans. KIEE 56 [9] (2007) 1602-1608.
8. L.J. van der Pauw, Philips Res. Repts. 13 (1958) 1-9.
9. M. Nader, F. Aldinger and M.J. Hoffmann, J. Mater. Sci. 34 (1999) 1197-1204.
10. Y.W. Kim, M. Mitomo, H. Emoto and J.G. Lee, J. Am. Ceram. Soc. 81 [12] (1998) 3136-3140.
11. Y.W. Kim, M. Mitomo and H. Hirotsuru, J. Am. Ceram. Soc. 80 [1] (1997) 99-105.
12. W. Wang, Z. Fu, H. Wang and R. Yuan, J. Eur. Ceram. Soc. 22 (2002) 1045-1049.
13. J. B. Hurst and S. Dutta, J. Am. Ceram. Soc. 70 [11] (1987) C303-C308.
14. A.L. Chamberlain, W.G. Fahrenholtz and G.E. Hilmas, J. Am. Ceram. Soc. 87 [6] (2004) 1170-1172.
15. A. Kondo, J. Ceram. Soc. Jpn., Int. Edition. 100 (1993) 1204-1208.
16. R. Landauer, J. Appl. Phys. 23 [7] (1952) 779-784.
17. Y.D. Shin, J.Y. Ju and J.S. Kwon, Trans. KIEE48C [2] (1999) 104-108.